A Simple Model of Lake Ontario's Coastal Boundary Layer

JOHN R. BENNETT AND ERIC J. LINDSTROM

Department of Earth and Planetary Sciences, Massachusetts Institute of Technology, Cambridge 02139

9 September 1976 and 4 March 1977

ABSTRACT

An empirical forced wave model of currents and thermocline displacements in the coastal zone of Lake Ontario is derived from data from the International Field Year for the Great Lakes (1972). The model consists of three linear wave equations for predicting the depth of the thermocline, its slope and the longshore volume transport from the wind. The empirical phase speeds are consistent with internal Kelvin wave and topographic wave theory and the response to a unit longshore wind stress is consistent with cross-section models of long lakes.

1. Introduction

Currents in the Great Lakes respond to the wind in a complex manner. While it is generally true that upwelling tends to occur at the shore to the left of the wind and that longshore currents tend to follow the wind direction, exceptions are common. In particular, during light winds current reversals and large changes in thermocline depth propagate counterclockwise around the shoreline. Striking examples of this were first documented by Mortimer (1963) for Lakes Michigan and Leman. Having only temperature and water level data, he interpreted them as internal Kelvin waves. The Lake Ontario measurements of Csanady and Scott (1974), however, show a more complicated pattern. The depth of the thermocline agrees with Kelvin wave theory (Clarke, 1977) but the reversals of the upper and lower layer currents do not occur simultaneously. Because of this, Csanady (1976) explained the observations as the sum of an internal Kelvin wave and a topographic wave.

Little quantitative analysis has been done on these waves, largely because of the limitations of Mortimer's Lake Michigan data consisting of temperature from municipal water intakes. The data of Csanady and Scott, however, are from daily synoptic surveys of temperature and current in five 10–15 km sections spaced evenly around the lake. Thus, while there are sampling errors in both time and longshore direction, there is considerable vertical and offshore resolution.

We chose the most complete series of their data, 15 July–15 August 1972, and fit it to a forced wave

Unauthenticated | Downloaded 09/11/24 07:51 PM UTC

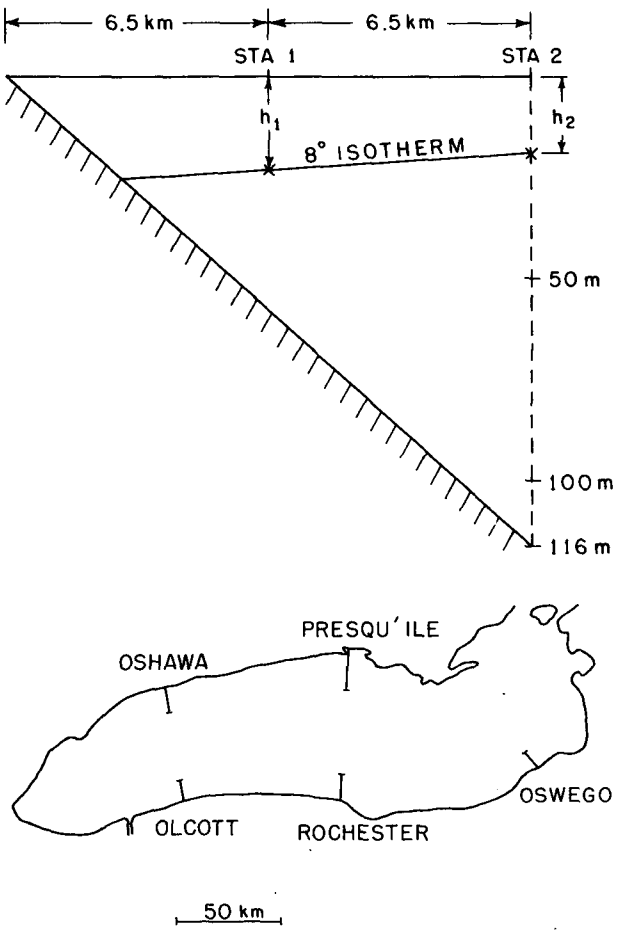

FIG. 1. An average shore zone of Lake Ontario (a) and the positions of the five coastal chains (b).

model to estimate the rate at which the waves are generated by the wind, the propagation speeds and the time it takes them to decay. We would like the forced wave model to complete with lakewide numerical models, and in a later paper will directly compare it to one. Our main goal is to describe the motion. However, since we would eventually like to understand the force balances as well, we will attempt to physically interpret the coefficients.

2. The model

Many theories of coastal flow can be reduced by separation of variables to the solution of first-order wave equations of the form

$$\frac{\partial A}{\partial t}+c\frac{\partial A}{\partial x}+\frac{A}{D}=\gamma\tau. \tag{1}$$

The dependent variable A will be anything we can easily estimate from the data. The independent variables are time t and arc length x; τ is the longshore component of the wind stress divided by water density. The three parameters c, D and γ are the phase velocity of free waves, the decay time and a wind generation coefficient.

The theories (Bennett, 1973; Gill and Clarke, 1974; Gill and Schumann, 1974; Clarke, 1977) assume that the frequency is small compared to the Coriolis parameter and the offshore scale is much smaller than the longshore scale; consequently the longshore component of the current is geostrophic and the offshore component of the wind is neglected. While some of the parameters can be estimated from this theory, it is easier to regard them as empirical for the moment and compare them with theory afterward.

To estimate the parameters we computed finite-difference solutions to the wave equation for $\gamma=1$ over a range of c and D and the correlation coefficient between the model and the data. The value of γ which minimizes the mean-square error is then

$$\gamma=r\frac{\sigma}{\sigma_M}, \tag{2}$$

where r is the correlation coefficient, and σ and σ_M are the standard deviations of the data and the model solution.

The model was run from the initial condition of zero at 1 July through 15 August. Since the first data are

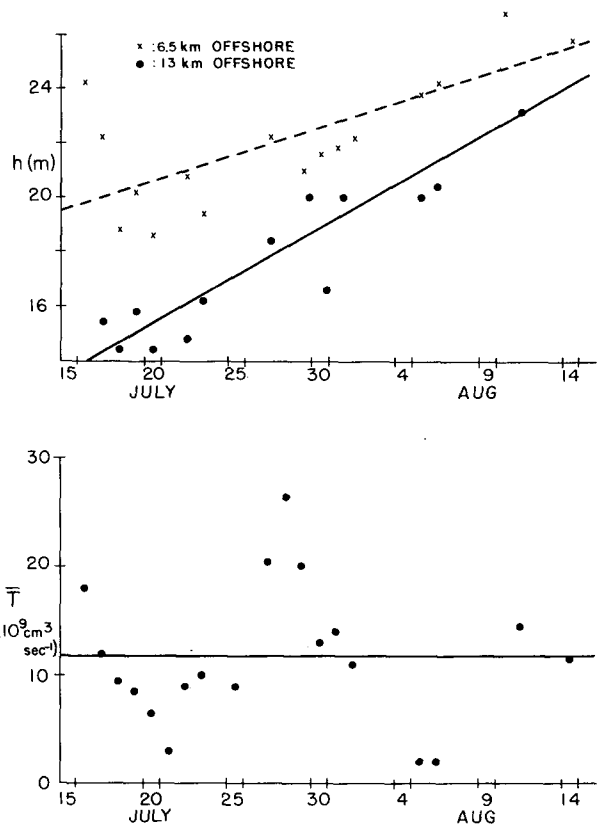

FIG. 2. Five-station averages of thermocline depth at 6.5 km and 13 km offshore.

Unauthenticated | Downloaded 09/11/24 07:51 PM UTC

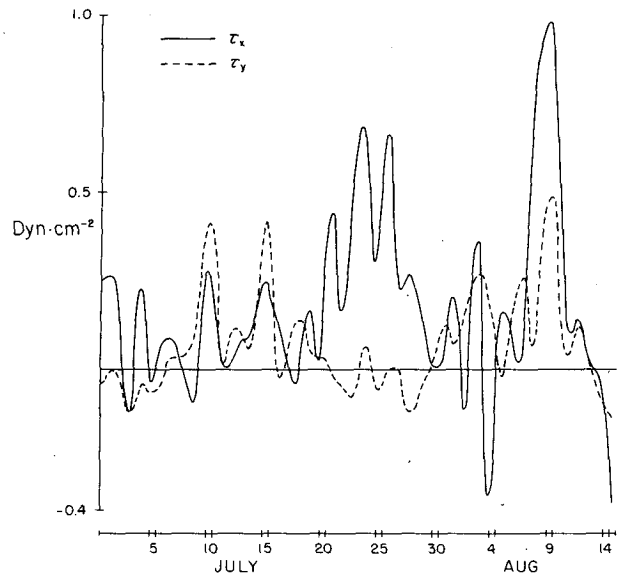

FIG. 3. Wind stress on Lake Ontario, 1 July–15 August 1972, computed from wind at 3 m at a mid-lake buoy.

from 15 July there are 14 days for the errors in the initial condition to decay. The numerical grid has 32 points spaced evenly around the perimeter of the lake and a time step of 3 h. The finite-difference scheme is

$$A^{n+1}=A^{n-1}\left(1-\frac{2\Delta t}{D}\right)-\frac{c\Delta t}{\Delta x}(A^n_{l+1}-A^n_{l-1})+2\tau\gamma\Delta t, \quad (3)$$

where $n=t/\Delta t$ and $l=x/\Delta x$. This formula is applied only to alternate points in space and time and the actual numbers compared with observations are averages over $2\Delta x$ and $2\Delta t$.

The coastal chain data were provided to us by J. T. Scott and G. T. Csanady in the form of hand-contoured temperature and longshore velocity sections and estimates of the longshore volume transport. The temperature sections were used to estimate the depth of the 8°C isotherm at two stations for each section, one at about the 50 m contour and the other at the end of the section. Fig. 1a illustrates an average shore zone and the average position of the 8°C isotherm. Fig. 1b shows the positions of the five coastal sections employed.

TABLE 1. Parameters of the forced wave models for thermocline depth H, thermocline slope S and longshore volume transport T.

	c (cm s^{-1})	D (days)	γ
H	30	5	6.4×10^{-3}s cm^{-1}
S	40	20	6.1×10^{-9}s cm^{-2}
T	60	10	2.6×10^{5} cm

Daily averages of the nearshore and offshore thermocline depths h_1 and h_2 for the days when all five coastal sections were made are given in Fig. 2a. Both show a seasonal deepening of about 0.3 m day^{-1}. In addition, the difference between them decreases, presumably due to the slow spin down of the spring thermal circulation. For the days when all five stations were available the average transport is given in Fig. 2b. The average of all these is 11.8×10^9 cm^3 s^{-1}. Since longshore transport here is defined as positive when the coast is on the right of the current, this is a cyclonic flow consistent with the mean thermocline slope. Since it is still unclear why this circulation persists so long into the summer (Pickett and Richards,

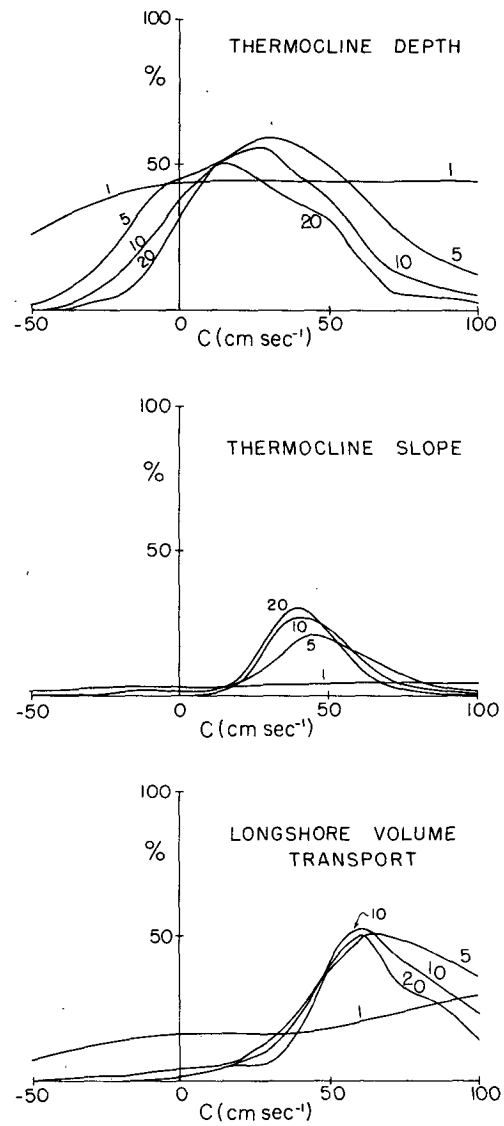

FIG. 4. Ratio of model of data variance for a forced wave model with phase velocity c and for decay times of 1, 5, 10 and 20 days.

Unauthenticated | Downloaded 09/11/24 07:51 PM UTC

1975; Bennet, 1975) and the model with a uniform wind stress cannot generate this mean pattern, we subtracted the thermocline trend lines and the mean transport from the data.

The two isotherm depths were then combined into two variables—H, the average thermocline depth and S, the thermocline slope—defined as

$$\left.\begin{aligned} H&=\frac{h_1+h_2}{2}\\ S&=\frac{h_1-h_2}{L}\end{aligned}\right\}, \tag{4}$$

where L, the distance between the two stations, is defined locally. The third variable is Scott's estimate of the volume transport T. For all three of these variables the sign convention is such that a longshore wind with the shore to the right would generate a positive value, i.e., we expect all three values of γ to be positive.

The longshore wind stress was computed from the local tangent to the shore and hourly stress values from a single mid-lake buoy (IFYGL station 10) provided by F. C. Elder of the Canada Centre for Inland Waters. Elder used the formula

$$\tau=1.5\times10^{-6}|\mathbf{W}|\mathbf{W}, \tag{5}$$

where $\mathbf{W}$ is the wind (cm s^{-1}). A smoothed version of stress is given in Fig. 3. There are two major pulses of wind from the west, 21–26 July and 9–10 August.

The ratio of model to data variance as a function of phase speed and decay time is shown in Fig. 4. This figure tells us which parameters work best and which parameters don't work. For example, the choice $c=0$ is simply an exponentially filtered local longshore wind stress. This model with a 1-day decay time can explain approximately 40% of thermocline depth, about 4% of thermocline slope and about 20% of the longshore transport variance. The three peak values, however, are 60, 30 and 50%, respectively.

The best choices of c, D and γ are given in Table 1. Fig. 5 compares these models with the data. Not much can be said about this figure; the fit of the model to nature is only good or bad in comparison with another model.

3. Physical interpretations

In effect we have now empirically derived the following equations of motion for Lake Ontario's coastal zone:

$$\frac{\partial H}{\partial t}+30\frac{\partial H}{\partial x}+\frac{H}{4.32\times10^5}=6.4\times10^{-3}\tau \tag{6}$$

$$\frac{\partial S}{\partial t}+40\frac{\partial S}{\partial x}+\frac{S}{17.3\times10^5}=6.5\times10^{-9}\tau \tag{7}$$

$$\frac{\partial T}{\partial t}+60\frac{\partial T}{\partial x}+\frac{T}{9.64\times10^5}=2.6\times10^5\tau. \tag{8}$$

Here the longshore wind stress is computed from (5) and all units are cgs. To test whether these parameters make physical sense we will now compare them with theory.

First, consider the effect of a unit longshore wind stress impulse $\tau_s=1$ dyn cm^{-2} acting for 10^5 s, and neglect wave propagation and friction. These equations predict that H would increase by 6.4 m, S would increase by 6.1×10^{-4} and T would increase by 2.6×10^{10} cm^3 s^{-1}. The increase in volume transport is about 20% of the wind's momentum flux across the 13 km wide surface. If the density difference across the thermocline were 10^{-3} the change in slope would give a geostrophic current shear of $\sim$6 cm s^{-1}. Even if the lower layer were stagnant this shear would account for about half the change in volume transport. The other half is presumably a current independent of depth. Since the two layers do not differ much in volume we conclude that roughly 15% of the wind's momentum flux goes into accelerating the water above the thermocline and about 5% goes into accelerating the water below the thermocline.

The cross-section theory of Bennett (1974) predicts that if bottom stress is neglected the fraction of the wind's momentum flux which goes into accelerating the water is $1-H/\bar{H}$, where H is the local depth and $\bar{H}$ the average depth of the lake. This fraction is about 37% for the average section of Fig. 1. However, when a quadratic bottom drag is included in the cross-section model, the volume transport increase in one day is only about half of this—consistent with the estimate of the forced wave model.

The fact that this longshore momentum budget balances and agrees with the cross-section theory is evidence that the wind stress coefficient of 1.5×10^{-6} is roughly correct. Another independent check on it comes from the mass balance of the shore zone. Referring to Fig. 1, if the average of h_1 and h_2 increases by 6 m and the slope increases by 0.6 m km^{-1}, then the area of the warm layer would increase by about 7×10^8 cm^2, a value again in rough agreement with the cross-section theory. In that theory this increase in upper layer volume is due to an Ekman drift of the surface water and a compensating return flow which has an offshore velocity independent of depth. This estimate of the response of the lake to a given wind impulse is smaller than the estimate of Csanady and Scott (1974). They concluded that nearly all the wind's momentum flux could be accounted for by the acceleration of the upper layer. Since they neglected the initial momentum of the water and analyzed only a few days of data, our estimate should clearly be preferred. It is not clear, however, whether this analysis can be refined to the point where it can

Unauthenticated | Downloaded 09/11/24 07:51 PM UTC

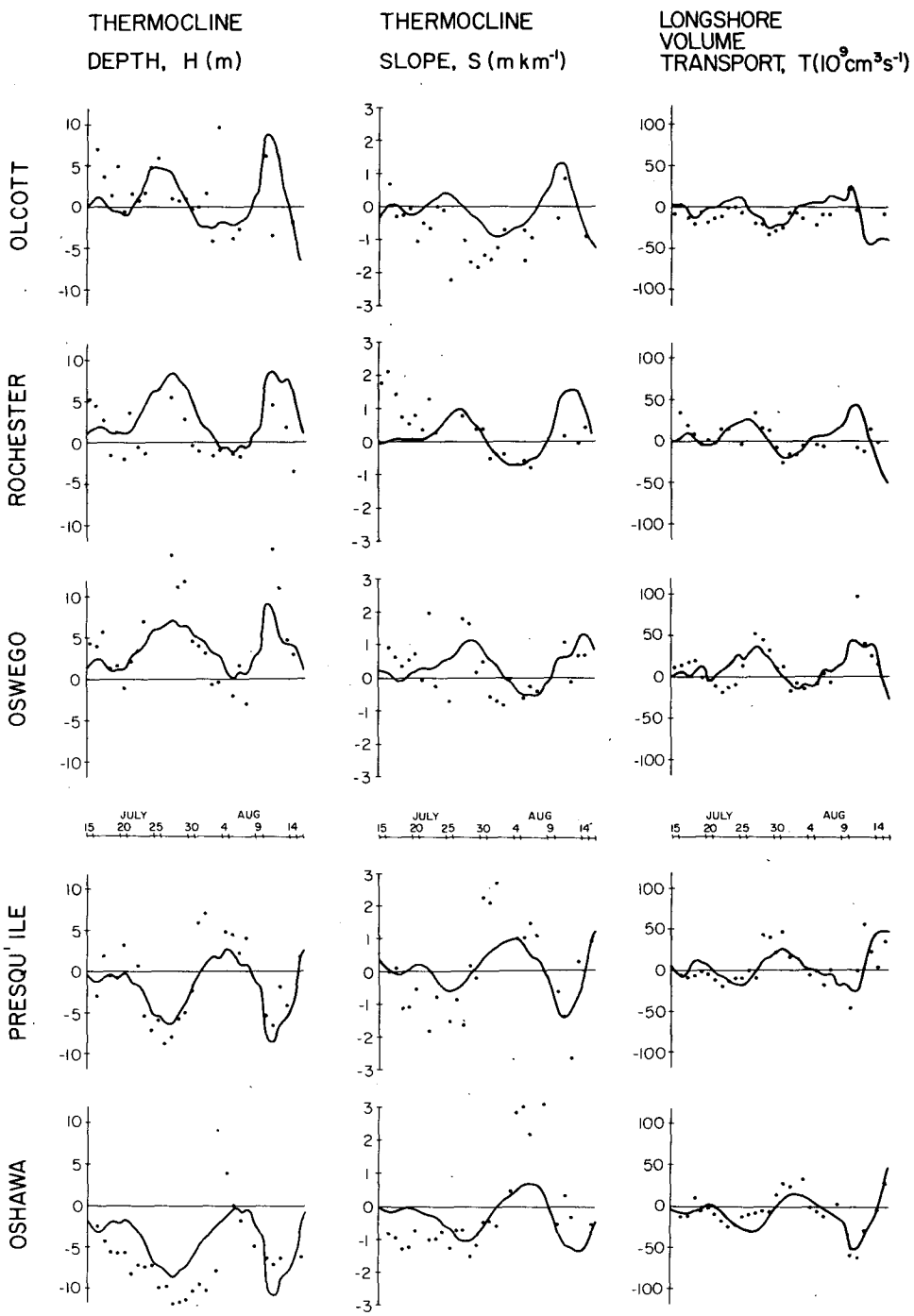

FIG. 5. Comparison of the best forced wave models of thermocline depth, thermocline slope and longshore volume transport to the daily observed values.

give estimates of the wind stress coefficient as good as those from water level data (Simons, 1976; Donelan *et al.*, 1974).

The thermocline depth and slope tend to propagate with a speed of 30–40 cm s^{-1} and the transport propagates at about 60 cm s^{-1}. These values are consistent with theoretical estimates for internal Kelvin and topographic waves. It is not possible, however, with these data to tell if the more advanced theories such as Wang's (1975) which include coupling between barotropic and baroclinic modes may give a better description. Likewise, we have not been able to im-

Unauthenticated | Downloaded 09/11/24 07:51 PM UTC

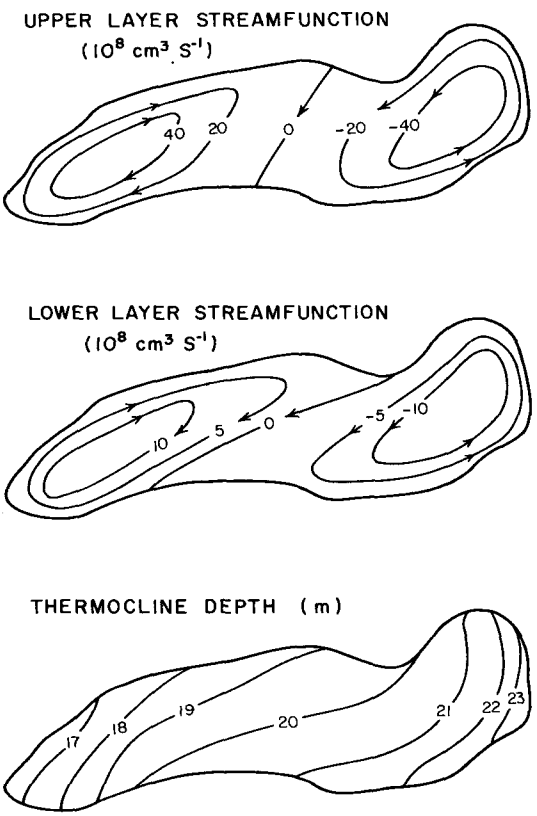

FIG. 6. Steady-state solution to the forced wave model for a uniform eastward wind stress of 0.1 dyn cm^{-2}.

prove the model by adding nonlinear terms as sug-tested by Bennett (1973).

To further examine the empirical equations we have computed their steady-state solutions. We then assumed that the longshore component of the flow obeys the thermal wind equation, the thermocline has an equilibrium depth of 20 m and there is a density difference of 10^{-3} across it. The three variables H, S and T are then sufficient to compute the longshore transport in both layers as functions of x. The flow in the interior of the lake then follows from mass continuity. The complete steady flow pattern for an eastward wind stress of 0.1 dyn cm^{-2} is given in Fig. 6. The circulation is a two-gyre pattern with the strongest currents to the left of the wind near the upwind and downwind shores as in the Birchfield (1972) theory. Further from shore the flow is opposite the wind in the lower layer and to the right of the wind in the upper layer. A phase shift occurs in the thermocline depth; offshore the maximum downward displacement occurs to right of the wind but nearshore it occurs directly downwind. The offshore slope of the thermocline is largest near the point where the longshore transport is largest. Thus, most of the flow is confined to the upper layer. Many of these features also occur in the three-dimensional numerical model which we are now in process of comparing with the forced wave model.

Acknowledgments. We thank T. J. Simons for his criticism. This work was supported by the Great Lakes Environmental Research Laboratory of the National Oceanic and Atmospheric Administration under Contract 03-022-57 and by a grant from the Henry L. and Grace Doherty Charitable Foundation.

REFERENCES

Bennett, J. R., 1973: A theory of large-amplitude Kelvin waves. *J. Phys. Oceanogr.*, **3**, 57–60.

——, 1974: On the dynamics of wind-driven lake currents. *J. Phys. Oceanogr.*, **4**, 400–414.

——, 1975: Another explanation of the observed cyclonic circulation of large lakes. *Limnol. Oceanogr.*, **20**, 108–110.

Birchfield, G. E., 1972: Theoretical aspects of wind-driven currents in a sea or lake of variable depth with no horizontal mixing. *J. Phys. Oceanogr.*, **2**, 355–366.

Clarke, A. J., 1977: Observational and numerical evidence for wind-forced coastal trapped long waves. *J. Phys. Oceanogr.*, **7**, 231–247.

Csanady, G. T., 1976: Topographic waves in Lake Ontario. *J. Phys. Oceanogr.*, **6**, 93–103.

——, and J. T. Scott, 1974: Baroclinic coastal jets in Lake Ontario during IFYGL. *J. Phys. Oceanogr.*, **4**, 524–541.

Donelan, M. A., F. C. Elder and P. F. Hamblin, 1974: Determination of the aerodynamic drag coefficient from wind set-up. *Int. Assoc. Great Lakes Res. Conf. Proc.*, **17**, 718–788.

Gill, A. E., and A. J. Clarke, 1974: Wind induced upwelling, coastal currents and sea-level changes. *Deep-Sea Res.*, **21**, 325–345.

——, and E. H. Schumann, 1974: The generation of long shelf waves by the wind. *J. Phys. Oceanogr.*, **4**, 83–90.

Mortimer, C. H., 1963: Frontiers in physical limnology, with particular reference to long waves in rotating basins. Publ. 10, Great Lakes Res. Div., University of Michigan, 9–42.

Pickett, R. L., and F. P. Richards, 1975: Lake Ontario mean temperatures and currents in July 1972. *J. Phys. Oceanogr.*, **5**, 775–781.

Simons, T. J., 1976: Effective wind stress over the Great Lakes derived from long-term numerical model simulations. *Atmosphere*, **13**, 169–179.

Wang, D-P., 1975: Coastal trapped waves in a baroclinic ocean. *J. Phys. Oceanogr.*, **5**, 326–333.

Unauthenticated | Downloaded 09/11/24 07:51 PM UTC